Electrical transport and Raman spectral studies of (110)-oriented PrBa2(Cu0.8M0.2)3O7 (M = Ga, Al, Zn, Ni) thin films

Hom Kandel, Tar-Pin Chen, Milko N. Iliev, Shawn Bourdo, Hye-Won Seo et al.

Citation: J. Appl. Phys. **113**, 143710 (2013); doi: 10.1063/1.4800829
View online: http://dx.doi.org/10.1063/1.4800829
View Table of Contents: http://jap.aip.org/resource/1/JAPIAU/v113/i14
Published by the American Institute of Physics.

Electrical transport and Raman spectral studies of (110)-oriented $PrBa_2(Cu_{0.8}M_{0.2})_3O_7$ (M = Ga, Al, Zn, Ni) thin films

Hom Kandel,[1] Tar-Pin Chen,[2] Milko N. Iliev,[3] Shawn Bourdo,[4] Hye-Won Seo,[2] Fumiya Watanabe,[4] and Tito Viswanathan[5]
[1]*National High Magnetic Field Laboratory, Florida State University, Tallahassee, Florida 32310, USA*
[2]*Department of Physics and Astronomy, University of Arkansas at Little Rock, Little Rock, Arkansas 72204, USA*
[3]*Texas Center for Superconductivity, University of Houston, Houston, Texas 77204, USA*
[4]*Center for Integrative Nanotechnology Sciences, University of Arkansas at Little Rock, Little Rock, Arkansas 72204, USA*
[5]*Department of Chemistry, University of Arkansas at Little Rock, Little Rock, Arkansas 72204, USA*

(Received 20 December 2012; accepted 25 March 2013; published online 11 April 2013)

The electrical transport and Raman spectral studies of (110)-oriented $PrBa_2(Cu_{0.8}M_{0.2})_3O_7$ (M = Ga, Al, Ni, Zn) (PBCMO) thin films have been investigated. The electrical resistivity, $\rho(T)$, of (110)-oriented $PrBa_2(Cu_{0.8}Ga_{0.2})_3O_7$ (PBCGO) and $PrBa_2(Cu_{0.8}Al_{0.2})_3O_7$ (PBCAO) thin films are many orders of magnitude higher than that of the (110)-oriented $PrBa_2Cu_3O_7$ (PBCO) thin films and follow Mott's 3D variable range hopping law up to room temperature. The electrical resistivity and Raman spectroscopic studies show that Al and Ga ions replace the Cu ions in the Cu-O chains of (110)-oriented PBCO and cause an extensive localization of charge carriers (holes) in the chains site of the PBCO. Our transport studies on $YBa_2Cu_3O_7$ (YBCO)/PBCGO and YBCO/PBCAO multilayers suggest that PBCAO and PBCGO thin films possess very less or no proximity effects. These results show (110)-oriented PBCGO and PBCAO thin films may serve as very effective insulators in YBCO based superconductor/insulator/superconductor tunneling Josephson junction. © *2013 AIP Publishing LLC*. [http://dx.doi.org/10.1063/1.4800829]

I. INTRODUCTION

$YBa_2Cu_3O_7$ (YBCO) based superconductor/insulator/superconductor (SIS) Josephson junctions are major components of superconducting electronics which could operate at liquid nitrogen temperature and avoid high cost and equipment complexity associated with using liquid helium. These devices may have I_cR_n products (with I_c is the junction critical current and R_n is the normal resistance) at least one order of magnitude larger than in the low temperature superconductor based junctions.[1] $PrBa_2Cu_3O_7$ (PBCO)[2–4] is considered to be the best insulating material for the fabrication of such junctions due to the excellent lattice match with YBCO, similar thin film fabrication conditions, and the same thermal expansion coefficients. However, the electrical resistivity of PBCO at 77 K is only about 200 Ω cm for bulk ceramic samples or ~0.01 Ω cm for nanometer thick layers, which is too low to provide a sufficient potential barrier for the junction unless its thickness is greater than ~200 nm.[5] With such a thick insulating layer; however, the Josephson current will be very low making the device unsuitable for many applications. In addition, proximity effect was observed in YBCO/PBCO bilayers and multilayers[6] which further decreased the insulating property of PBCO. The temperature dependence of the critical current density, $J_c(T) \sim (1 - T/T_c)^2$, displayed a typical superconducting/normal/superconducting (SNS)—type behavior in YBCO/PBCO/YBCO trilayer junction.[2] This showed that PBCO cannot serve as an effective insulator and a better insulating material is needed.

High-T_c SIS or SNS junctions have been fabricated using the c-axis or a-axis oriented PBCO,[2] Co-doped PBCO,[4] Ga-doped YBCO,[7] and Ga-doped PBCO[8–10] thin films in ramp-type and trilayer sandwich-type geometry. In the ramp-type junctions based on thin insulating layers of Ga-doped PBCO,[8,9] the J_c homogeneity was limited by the growth control of this barrier layer on the ramp. For 8 nm thick and 40% Ga doped samples, the I_cR_n values reached only 8 mV and none of these junctions had T_c-values higher than 50 K.[9] A proximity effect was observed in the ramp edge junction based on Ga doped YBCO barrier layer. The electrical resistivity of the barrier layer was 70 μΩ cm on 200 nm thick 7% Ga-doped YBCO sample. A considerable problem of the ramp-edge technology is its need for a well defined barrier growth on the edge in order to obtain a high reproducibility. On the other hand, a controllable, reproducible fabrication of non-hysteretic Josephson devices which operate at temperatures up to 80 K have been patterned from *in situ* deposited a-axis oriented YBCO/PBCO/YBCO trilayer junctions.[3]

Usually, [001]-axis (c-axis) or [100]-axis (a-axis) PBCO or few metals doped PBCO thin films have been studied, but the (110)–oriented metals doped PBCO thin films have not been investigated yet. In this context, we expect that the study of (110)–oriented PBCMO (M = Ga, Al, Ni, Zn) thin films will be very useful for the fabrication of well controlled and reproducible trilayer sandwich type SIS Josephson junctions. Using (110)–oriented thin film in SIS junction has following advantages: first, it employs a layered structure with the junction normal to the substrate surface with the c-axis of

the film lying in the plane of the substrate, while the diagonals of the a- and b-axis being perpendicular to the plane. This allows YBCO films to grow on top of the PBCMO (M = Ga, Al, Ni, Zn) films with the same orientation and take an advantage of longer coherence length along the CuO_2 planes. Second, the (110)-orientation films reveal a unique macroscopic in-plane alignment of their c-axis parallel to the [001] direction of the substrate contrary to the a-axis oriented thin films (i.e., with the a-axis perpendicular to the substrate surface) which have their c-axis randomly aligned either parallel to the [100] or to the [010] direction of the substrate, thus leading to 90° grain boundaries.[11]

In this paper, we report the electrical transport and Raman spectral properties of (110)-oriented PBCMO (M = Ga, Al, Ni, Zn) thin films grown on (110)-oriented $LaAlO_3$ (LAO) single crystal substrates. Our goal in this study is to find an excellent insulating material for the fabrication of YBCO SIS trilayer Josephson junction.

II. EXPERIMENT

Polycrystalline bulk materials of $PrBa_2[Cu_{0.8}M_{0.2}]_3O_7$ (M = Ga, Al, Ni, Zn) were synthesized by the solid state reaction method by mixing high purity Pr_6O_{11} (99.9%), CuO (99.7%), $BaCO_3$ (99.95%), Ga_2O_3 (99.9%), Al_2O_3 (99.9%), NiO (99.7%), and ZnO (99.9%) in appropriate proportions. The chemical powders as received from Alpha Aesar were mixed and ground thoroughly and were fired in an electric furnace at 950 °C for 48 h followed by cooling to room temperature. The fired samples were reground into the powders and structure and purity of the powders were checked by x-ray diffraction (XRD). The powders were carefully reground and the processes were repeated until the desired single phase was achieved. The single phase powders were then pressed into the 2.54 cm diameter ceramic discs (targets) using hydraulic press and then sintered in electric furnace at 925 °C for 24 h followed by an additional annealing process at 450 °C for another 24 h.

We deposited PBCMO (M = Ga, Al, Ni, Zn) thin films on (110)-oriented LAO using the pulsed laser deposition (PLD) technique [KrF excimer laser, 25 ns FWHM, repetition rate 3 Hz, energy density 1.0 J/cm^2]. The base vacuum of the system was 5×10^{-6} Torr and the target to substrate distance was 4 cm. The films were deposited in an O_2 atmosphere at a pressure of 500 mTorr at a temperature of 750 °C with the growth rate ~0.3 nm/s. The deposition was followed by 30 min annealing at a substrate temperature of 500 °C in one atmosphere O_2 pressure.

We also deposited 3-layers (Y/P/Y), 5-layers (Y/P/Y/P/Y), and 7-layers (Y/P/Y/P/Y/P/Y) multilayers, where Y represents YBCO and P represents $PrBa_2(Cu_{0.8}Ga_{0.2})_3O_7$ (PBCGO) or $PrBa_2(Cu_{0.8}Al_{0.2})_3O_7$ (PBCAO), respectively, on LAO (110) substrates using the PLD system equipped with a multi-target holder. The system was integrated to allow different targets to be placed in the beam of pulsed lasers and perform their ablation alternatively. The deposition parameters were similar to those applied in PBCMO (M = Ga, Al, Ni, Zn) thin film deposition. After the deposition of the each layer, the deposition process was interrupted for about 90 s to allow the films relax and improve the morphology of the multilayers.

X-ray diffraction of the thin film samples were carried out with Rigaku diffractometer using Cu K_α source radiation. Atomic force microscopy (AFM) was performed in tapping mode with the Veeco dimension 3100 instrument. Electrical resistivity measurements were performed in a liquid helium cryostat using standard DC four probe techniques. Raman spectra were obtained using Horiba Jobin Yvon T64000 Triple Raman Spectrometer equipped with a liquid nitrogen cooled charge coupled device (CCD) and a microscope in conjunction with computer-controlled XYZ stage and an optical cryostat microstat (Oxford instruments). The 488 nm and 633 nm lines of lasers were used for the excitation at a power of 0.21 MW under the 100× objective. The parallel scattering configurations [(001), (001)] = zz or [(110,110] = x′x′ which means that both incident and scattered light polarizations were parallel to either the (zz) or (x′x′) dimension of the substrate.

III. RESULTS AND DISCUSSION

The XRD pattern indicated that all the PBCMO (M = Ga, Al, Ni, Zn) thin films had (110) epitaxy without any detectable second phases [see Fig. 1].

AFM measurements showed RMS roughness ~6 nm in a $5 \times 5\ \mu$m scan on ~600 nm thick PBCMO thin films [see Fig. 2]. All the thin films were crack-free and consisted of elongated grains forming an oval pattern that ran along the (001) axis of the substrate. These patterns were significantly different than the square islands or spiral growth types generally observed in c-axis oriented films.

The electrical resistivities of the (110)-oriented PBCMO thin films at various temperatures are given in Fig. 3 and Table I. The electrical resistivity values of these thin film samples are ranked in the increasing order of $PrBa_2(Cu_{0.8}Ni_{0.2})_3O_7$ (PBCNO), $PrBa_2(Cu_{0.8}Zn_{0.2})_3O_7$ (PBCZO), PBCAO, and PBCGO, respectively. The resistivities of (110)-oriented PBCNO and PBCZO thin films are almost similar to that of (110)-oriented PBCO thin films. At 77 K, the resistivity of 20% Al and Ga doped (110)-oriented PBCO thin film samples are four to five orders higher in magnitude than in the (110)-oriented PBCO thin films. The difference in resistivity between undoped PBCO thin films and 20% Ga or Al doped PBCO thin film is tremendously large at low temperatures. For example, at 40 K, the resistivity values of (110)-oriented PBCO, PBCAO, and PBCGO thin films are 37.63 Ω cm, 6.03×10^7 Ω cm, and 1.33×10^9 Ω cm, respectively.

The plot of the natural logarithm of the resistivity against $T^{-1/4}$ for (110)-oriented PBCMO thin films follows the Mott's 3D variable range hopping law (VRH)

$$\rho(T) = \rho_0 \exp(T_0/T)^{1/4}, \quad (1)$$

where T_0 and ρ_0 are material constants. According to Mott's law, T_0 is given by the relation

$$T_0 = \frac{\beta}{[K_B N(E_F) a^3]}, \quad (2)$$

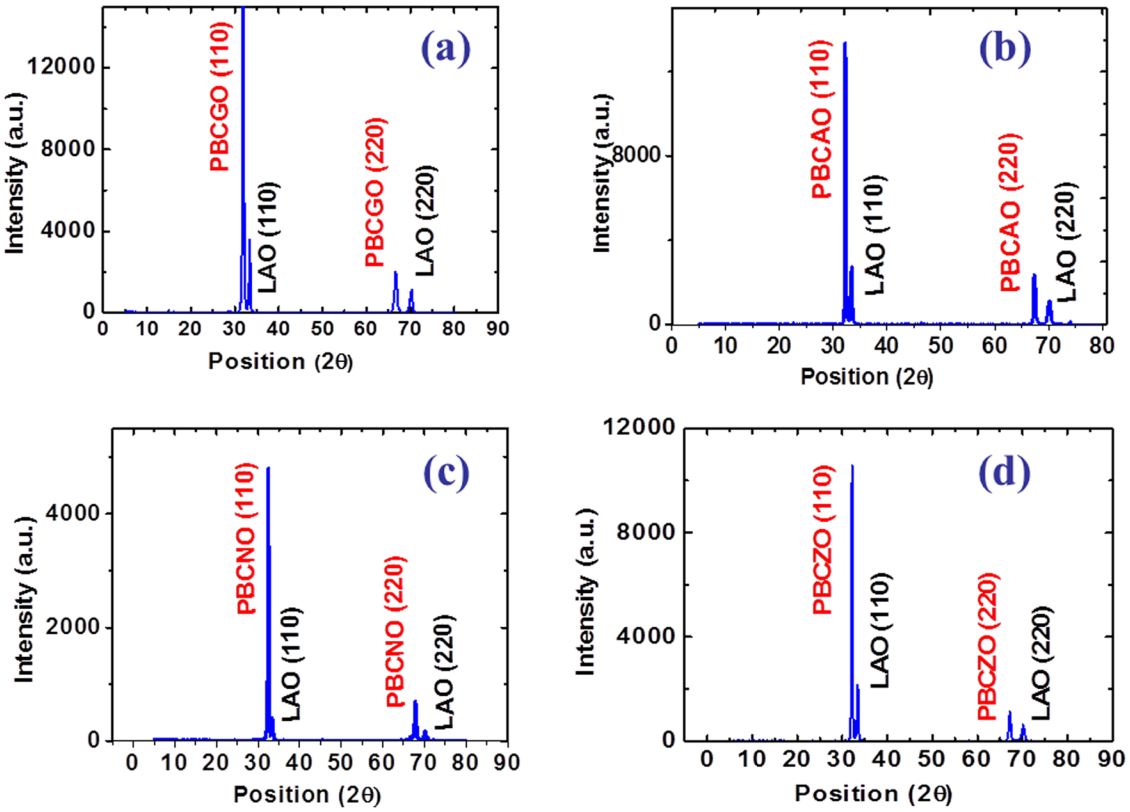

FIG. 1. XRD pattern of (110)-oriented (a) PBCGO, (b) PBCAO, (c) PBCNO, and (d) PBCZO thin films.

where $N(E_F)$ is the density of the states at the Fermi level, a is the localization radius of the states near the Fermi level, K_B is the Boltzmann constant, and β is a numerical coefficient with its value ~20.[12] As shown in the Fig. 4, the linear relation exists up to room temperature in (110)-oriented PBCAO and PBCGO thin films indicating localization starts from room temperature in (110)-oriented PBCAO and PBCGO thin films. However, the linear relation exists only up to 100 K in (110)-oriented PBCO thin films, 120 K in (110)-oriented PBCNO, and 140 K in (110)-oriented PBCZO. From these plots, the fitting parameters ρ_0 and T_0 have been calculated (see Table II). These values for PBCO are in close agreement with the values in the literature.[13] We see a sharp increase in T_0 values in (110)-oriented PBCAO and PBCGO thin films which indicates a decrease in either the density of states at the Fermi level or localization length "a" or the both in these samples.

The localization parameters such as localization radius (a), activation bandwidth (activation energy for hopping ($\varepsilon_0(T)$), and average hopping distance (R) were calculated using the following formulae and are shown in the Table II:

$$a = [\beta/K_B T_0 N(E_F)]^{1/3}, \tag{3}$$

$$\varepsilon_0(T) \sim [d\ln(\rho)/d(K_B T)^{-1})] = (K_B T)^{3/4}(K_B T_0/\beta)^{1/4}, \tag{4}$$

$$R = a(T_0/T)^{1/4}. \tag{5}$$

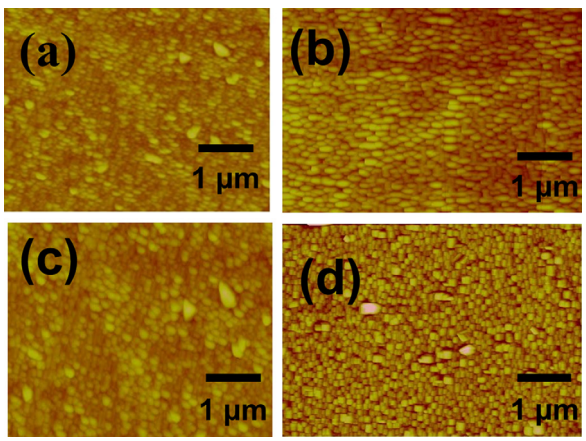

FIG. 2. AFM images of (110)-oriented (a) PBCAO, (b) PBCGO, (c) PBCZO, and (d) PBCNO thin films.

Using Eq. (4), the half activation bandwidths for (110)-oriented PBCAO and PBCGO thin films were determined to be 327 meV and ~352 meV at 300 K and 72 meV and 78 meV at 40 K, respectively, indicating that the hopping is mainly thermally assisted. The average hopping distances for (110)-oriented PBCAO and PBCGO thin films were determined to be 2.3 nm and 1.7 nm at 300 K and 3.9 nm and 3.7 nm at 40 K, respectively. The increase of the average hopping distances and decrease of activation energies with a reduction of the temperature are typical for conduction by VRH between localized states. This is a result of VRH being controlled by two opposing requirements: (1) minimization of the hopping distance to increase the overlap probability of the electron wave functions and (2) the preference of the electrons to jump to a distant site with the same energy level to minimize the activation energy. Consequently, this

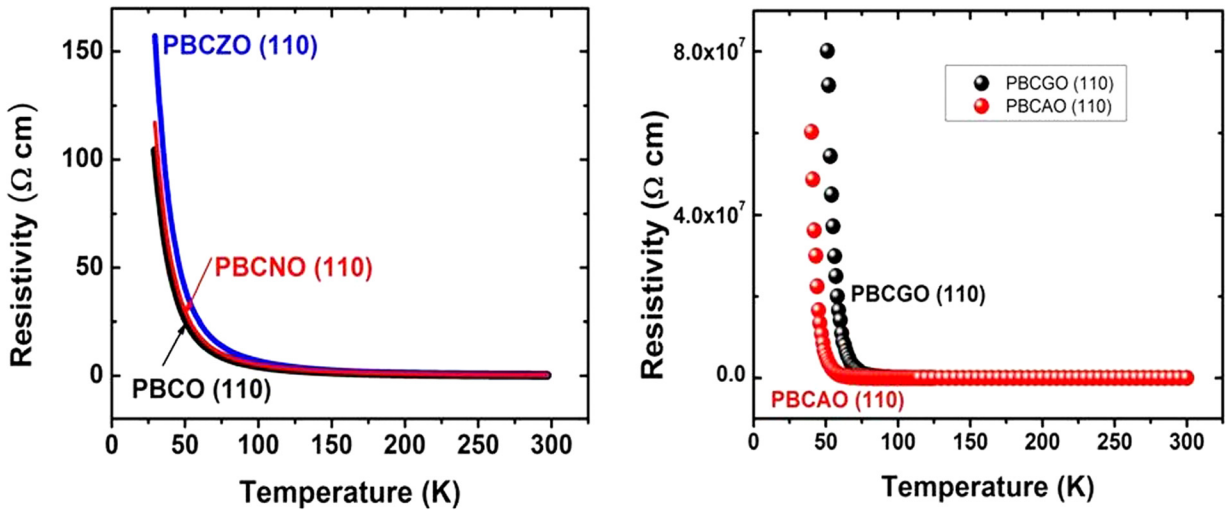

FIG. 3. Electrical resistivity of (a) (110)-oriented PBCO and PBCMO (M = Ni and Zn) thin film and (b) (110)-oriented PBCMO (M = Al and Ga) thin films.

increases the hopping distance and decreases the activation energy with the lowering of the temperature.

Thus, the hopping conductivity in (110)-oriented PBCAO and PBCAO thin films indicate that electronic states are extensively localized at the Fermi energy by some kind of disorder introduced by dopants Ga and Al (which behave as impurities).

We performed Raman spectroscopy to study the location of the dopants. As the dopants differ from the Cu ions typically used, they may break crystal symmetry and cause the inactive Raman mode to become active. The Raman spectra for (110)-oriented PBCO and PBCMO (M = Ga, Al, Ni, Zn) are shown in Fig. 5. The Raman modes at approximately 600 cm^{-1} shown in Figs. 5(b) and 5(c) for the (110)-oriented PBCAO or PBCGO does not appear in spectrum of (110)-oriented PBCO as shown in Fig. 5(b) or (110)-oriented PBCNO and PBCZO thin films as shown in the Figs. 5(d) and 5(e). As this mode is the breathing mode of the Cu-O chain and is Raman inactive but infrared (IR) active, it does not occur in the Raman spectrum of PBCO. However, the existence of this mode in both the Al- and Ga-doped thin films indicates that some of the Cu ions in the Cu-O chain were replaced by Al and Ga and chain symmetry was subsequently broken. As a result of broken symmetry, the IR active mode becomes a Raman active mode and provides strong evidence than some, if not all, of the Al and Ga ions replaced the Cu ions in the Cu(1) or chain sites.

It is generally accepted that superconductivity for 123-cuprates is from the CuO_2 planes and the Cu-O chains serve as reservoirs for superconducting electrons. Based on the optical reflectivity data of Takenaka *et al.*[14] and using their own electronic structure calculations, Fehrenbacher and Rice[15] argued that the 2p holes in O from the Cu(2) or plane sites in PBCO are pulled toward the Pr ions, and thus, the CuO_2 planes in PBCO are non-superconducting. Therefore, PBCO becomes insulating material even though its Cu-O chains are still conducting. Combining both Raman and electrical resistivity studies, we argue that the Al and Ga ions replace the Cu ions and not only break the symmetry of the chains but also localize the charge carriers (holes) and destroy the conduction in the Cu-O chains locally. For this reason, the electrical resistivities of Al and Ga doped PBCO samples are sharply higher.

As the Ga- and Al-doped samples had the highest electrical resistivity, we chose these for the purpose of studying the proximity effect in PBCMO (M = Al, Ga)/YBCO multilayers and fabricated 3-layer (Y/P/Y, where Y represents YBCO and P represents PBCMO), 5-layer (Y/P/Y/P/Y), and 7-layer (Y/P/Y/P/Y/P/Y) multilayers. Previous experimental data on YBCO/PBCO multilayers[6,16] indicated that for a

TABLE I. Electrical resistivity values of (110)-oriented PBCO and PBCMO (M = Ni, Zn, Al, Ga) thin films at 300 K and 77 K.

Sample	ρ_{300K} (Ω cm)	ρ_{77K} (Ω cm)
PBCO (110)	0.23	8.5
PBCNO (110)	0.33	9.5
PBCZO (110)	0.39	11.8
PBCAO (110)	3.40	6.96×10^4
PBCGO (110)	8.20	8.91×10^5

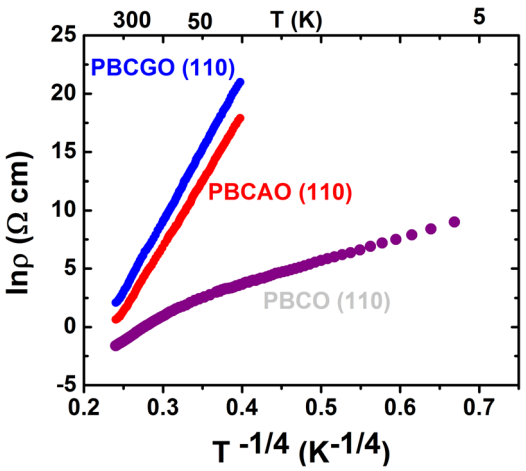

FIG. 4. ln ρ vs. $T^{-1/4}$ for (110)-oriented PBCO, PBCAO, and PBCGO thin films.

TABLE II. Various localization parameters of (110)-oriented PBCO, PBCAO, and PBCGO thin films.

Sample	ρ_0 (Ω cm)	T_0 (K)	Localization radius (nm)	Activation energy at 77 K (meV)
PBCO (110)	4.4×10^{-5}	1.9×10^{5}	0.8	23
PBCO (110)	3.2×10^{-12}	1.55×10^{8}	0.09	117
PBCAO (110)	6.47×10^{-12}	2.08×10^{8}	0.08	127

given thickness of YBCO film, T_c of the multilayers decreases with increasing thickness of the PBCO layers. The results can be explained by the existence of proximity effect between the YBCO superconductor layer and the PBCO semiconductor layer. Migration of the superconducting electrons from the YBCO film to the PBCO film lowers the superconducting electron density in the multilayer systems and thus T_c decreases. For each multilayers, we used 20 nm thick YBCO films and 20% Al- or Ga-doped PBCO films of varying thickness for different multilayers. We measured each multilayer's electrical resistivity as a function of temperature.

Figs. 6(a) and 6(b) show the plotted resistivity data for the 20 nm thick YBCO films in YBCO/PBCGO/YBCO and YBCO/PBCAO/YBCO trilayers, respectively. These figures show that all curves drop at the same temperature regardless of the thickness of the actual PBCGO or PBCAO layers in the various trilayers. This demonstrates that the onset T_c of all trilayers was the same and indicates that very small or no proximity effect occurred between the YBCO and PBCGO or PBCAO films. These figures also show that the T_c values for the trilayers (YBCO/PBCGO/YBCO) or (YBCO/PBCAO/YBCO) are same for 1.25 nm or 20 nm PBCGO or PBCAO thin films. From this, we conclude that the 1.25 nm PBCMO (M = Ga or Al) films provide the same insulating effect as the 20 nm PBCMO (M = Ga or Al) films and are capable of serving as good tunneling barriers for YBCO SIS trilayer Josephson junction device.

IV. CONCLUSIONS

In conclusion, (110)-oriented PBCGO and PBCAO thin films were most insulating out of the four different metals doped (110)-oriented PBCMO (M = Ga, Al, Ni, and Zn) thin films. The electrical transport mechanism of the (110)-oriented PBCGO films is via the 3D VRH among the localized states. Substitution of Cu (1) with Ga and Al ions in (110)-oriented PBCO have caused the extensive localization of charge carriers (holes) in the Cu-O chains. From the Raman spectroscopic studies, we were able to determine that

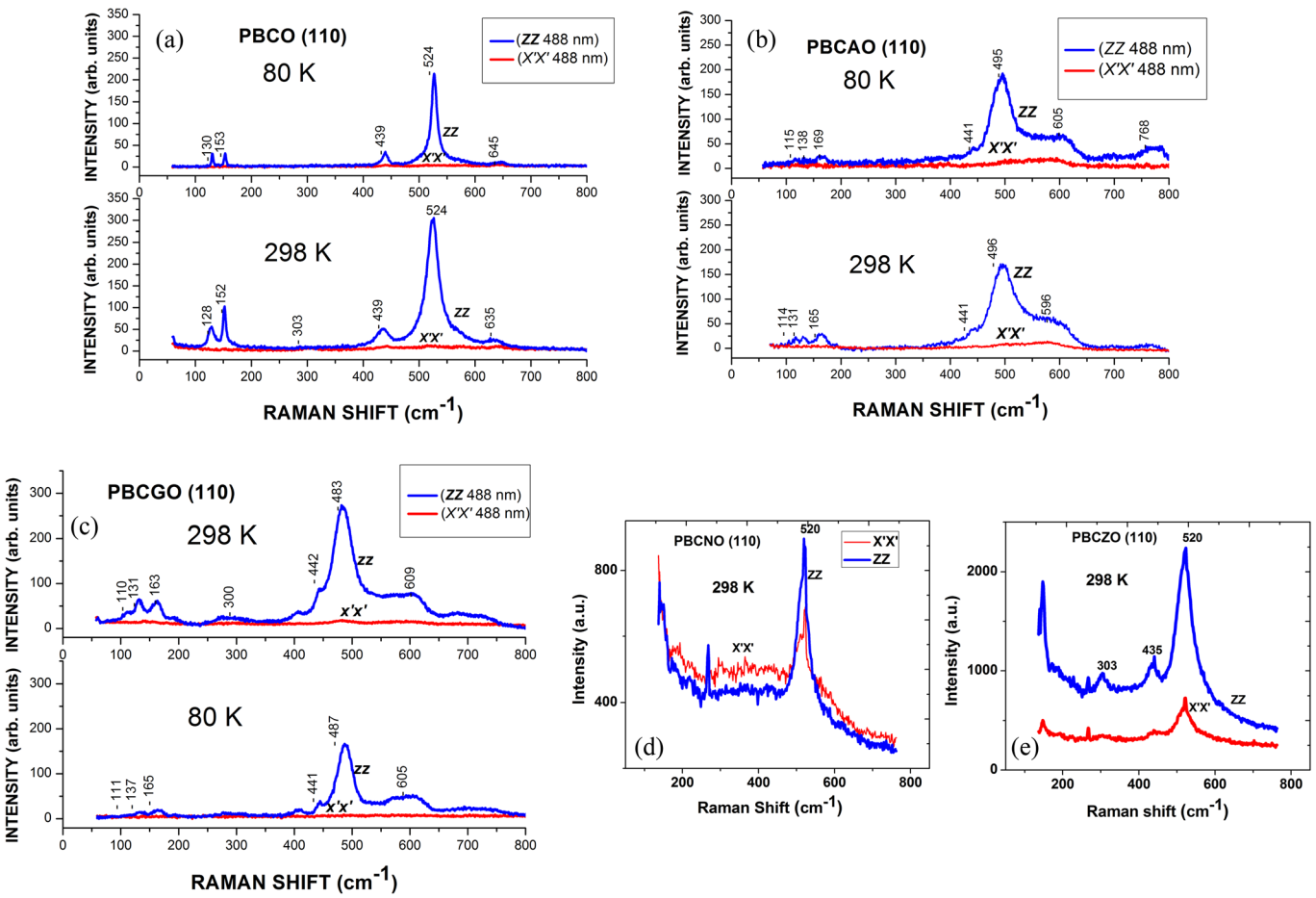

FIG. 5. (a) Polarized Raman spectra of (110)-oriented PBCO thin films at 298 K and 80 K with 488 nm laser excitation. (b) Polarized Raman spectra of (110)-oriented 20% Al doped PBCO thin films at 298 K and 80 K with 488 nm laser excitation. (c) Polarized Raman spectra of (110)-oriented 20% Ga doped PBCO thin films at 298 K and 80 K with 488 nm laser excitation. (d) Polarized Raman spectra of (110)-oriented 20% Ni doped PBCO thin film at 298 K. (e) Polarized Raman spectra of (110)-oriented 20% Zn doped PBCO thin film at 298 K.

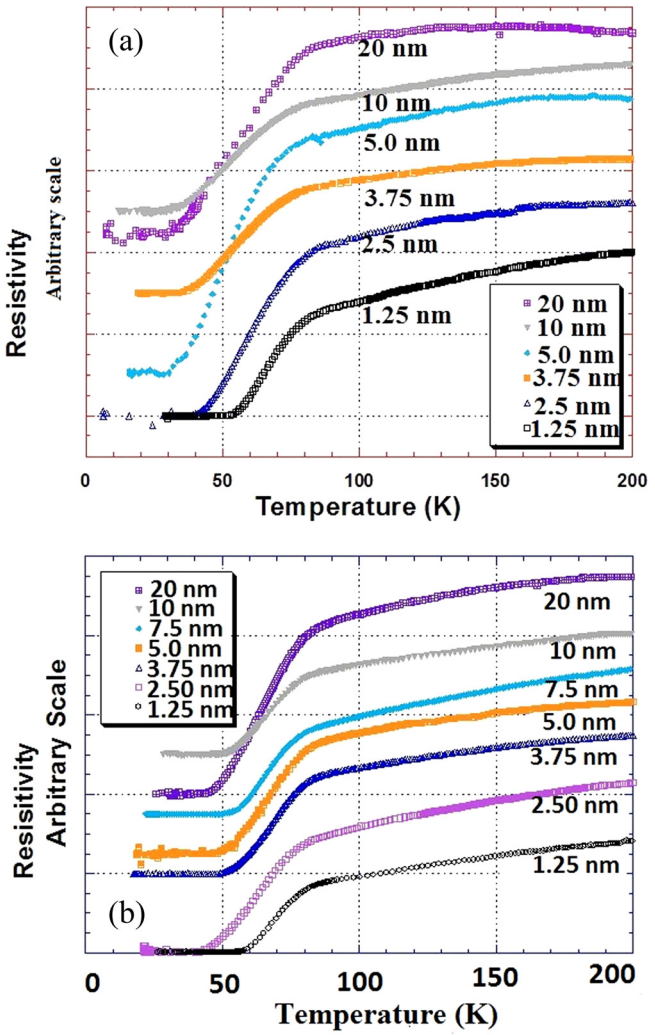

FIG. 6. (a) Plot of resistivity against Temperature for YBCO/PBCGO/YBCO trilayers. The thickness of YBCO layers are 20 nm, while the thickness of PBCGO layers vary from 1.25 nm up to 20 nm in the trilayers. An arbitrary scale has been used to represent the relative values of resistivities for six trilayers which contain varying thickness of PBCGO layers (1.25 nm, 2.5 nm, 3.75 nm, 5.0 nm, 10 nm, and 20 nm). (b) Plot of resistivity against Temperature for YBCO/PBCAO/YBCO trilayers. The thickness of YBCO layers are 20 nm while the thickness of PBCGO layers vary from 1.25 nm up to 20 nm in the trilayers. An arbitrary scale has been used to represent the relative values of resistivities for six trilayers which contain varying thickness of PBCAO layers (1.25 nm, 2.5 nm, 3.75 nm, 5.0 nm, 10 nm, and 20 nm).

at least some of the Al and Ga ions replaced Cu ions in the Cu-O chains in (110)-oriented PBCGO and PBCAO thin films. The resulting replacements broke the symmetry of the Cu-O chains and created disorder and charge localization in the Cu-O chains causing a drastic increase in the electrical resistivity of these samples. Very small or no proximity effect was observed in YBCO/PBCGO and YBCO/PBCAO multilayers.

In view of very high electrical resistivity, very small or no proximity effect, and structural and chemical compatibility, (110)-oriented PBCO and PBCGO thin films may serve as effective insulators in YBCO SIS trilayer Josephson junctions.

ACKNOWLEDGMENTS

The authors wish to thank S. Z. Wang for his technical assistance in experimental setup of the pulsed laser deposition system.

[1]D. Stornaiuolo, G. Papari, N. Cennamo, F. Carillo, L. Longobardi, D. Massarotti, A. Barone, and F. Tafuri, Supercond. Sci. Tech. **24**, 045008 (2011).
[2]J. Gao, Y. Boguslavkij, B. Klopman, D. Terpstra, G. Gerritsma, and H. Rogalla, Appl. Phys. Lett. **59**, 2754 (1991).
[3]J. Barner, C. T. Rogers, A. Inam, R. Ramesh, and S. Bersey, Appl. Phys. Lett. **59**, 742 (1991).
[4]M. Sato, G. Alvarez, T. Utagawa, K. Tanabe, and T. Morishita, Jpn. J. Appl. Phys. **41**, 5572 (2002).
[5]J. L. Peng, P. Klavins, R. N. Shelton, H. B. Radousky, P. A. Hahn, and L. Bernardez, Phys. Rev. B **40**, 4517 (1989).
[6]Q. Li, X. Xi, D. Wu, A. Inam, S.Vadlamannati, R. Ramesh, D. M. Hwang, J. A. Martinez, and L. Nazar, Phys. Rev. Lett. **64**, 3086 (1990).
[7]I. H. Song, E. H. Lee, B. M. Kim, I. Song, and G. Park, Appl. Phys. Lett. **74**, 2053 (1999).
[8]K. Verbist, O. I. Lebedev, G. Van Tendeloo M. A. J. Verhoeven, A. J. H. M. Rijnders, D. H. A. Blank, and H. Rogalla, Appl. Phys. Lett. **70**, 1167 (1997).
[9]M. A. J. Verhoeven, G. J. Gerritsma, H. Rogalla, and A. A. Golubov, Appl. Phys. Lett. **69**, 848 (1996).
[10]N. Bergeal, J. Lesueur, M. Sirena, G. Faini, M. Aprili, J. P. Courton, and B. Leridon, J. Appl. Phys. **102**, 083903 (2007).
[11]J. Brunen, T. Scratch, J. Zegenhagen, and M. Cardona, Physica C **289**, 177 (1997).
[12]B. I. Shklovskii and A. L. Efros, *Electronic Properties of Doped Semiconductors* (Springer-Verlag, Berlin, 1984).
[13]B. Fisher, J. Genosaar, L. Patlagon, and A. B. Kaiser, Phys. Rev. B **50**, 4118 (1994).
[14]K. Takenaka *et al.*, Phys. Rev. B **46**, 5833 (1992).
[15]R. Fehrenbacher and T. M. Rice, Phys. Rev. Lett. **70**, 3471 (1993).
[16]D. H. Lowndes, D. P. Norton, and J. D. Budal, Phys. Rev. Lett. **65**, 1160 (1990).